Optical and Quantum Electronics (2024) 56:582
https://doi.org/10.1007/s11082-023-06261-y

Preparation, crystal structure and physicochemical properties of nickel (II) nitrate hexahydrate boric acid: an efficient for nonlinear optical activity

V. Selvarani[1] · P. Jayaprakash[2] · P. Ravichandran[3] · P. Shenbagarajan[2] · T. C. Sabari Girisun[4] · S. Selvaraj[5]

Received: 25 September 2023 / Accepted: 30 December 2023 / Published online: 30 January 2024

Abstract

The invention discloses a preparation method for nickel (II) nitrate hexahydrate boric acid and the growth of single crystals by the slow evaporation solution growth technique. Single crystal x-ray diffraction (XRD) analysis shows N2NHB crystallize in triclinic P crystal system with lattice parameters of a = 6.61 Å, b = 7.05 Å, c = 7.07 Å, α = 119.61°, β = 92.25°, γ = 101.11° and volume = 278 Å^3. The chemical composition and the corresponding functional groups of the grown crystal have been identified by EDAX and FTIR analyses. Scanning electron microscope (SEM) pictograph indicated that the particles were closely spherical in shape with slight agglomeration. UV–Visible studies shows N2NHB crystal exhibit lower cut-off wavelength of 314 nm, wide optical window (320 – 800 nm) and wide band gap of 4.16 eV. According to the fluorescence spectrum, the emission occurs at a wavelength of 533 nm. Different temperatures were used to study the Grown crystalc dielectric behaviour. A positive photocurrent is found in the Grown crystal, as shown by the photoconductivity analysis. The second harmonic generation (SHG) capability was demonstrated by the standard Kurtz and Perry powder method. Open aperture Z-scan technique reveals that the material exhibits two-photon absorption phenomenon with nonlinear absorption coefficient of 0.75×10^{-11} m/W. The material displays optical limiting behaviour with an onset limiting threshold of 4.72×10^{12} W/m^2. Altogether the grown N2NHB crystal can be utilized wide variety of optoelectronic applications of which optical limiting activity for laser safety devices is notable.

✉ P. Jayaprakash
jayajp85@gmail.com

[1] Department of Chemistry, St. Joseph's Institute of Technology, OMR, Chennai 600119, TamilNadu, India

[2] Department of Physics, St. Joseph's Institute of Technology, Tamil Nadu, OMR, Chennai 600119, India

[3] Department of Chemical Engineering, St. Joseph's Institute of Technology, Tamil Nadu, OMR, Chennai 600119, India

[4] Nanophotonics Laboratory, Department of Physics, Bharathidasan University, Tiruchirappalli 620024, Tamil Nadu, India

[5] Department of Physics, Saveetha School of Engineering, Saveetha Institute of Medical and Technical Sciences, Thandalam, Chennai 602105, Tamil Nadu, India

Keywords NLO · Crystal growth · EDAX · Photoconductivity · Optical limiting

1 Introduction

In current research, the most promising direction for nonlinear optical (NLO) materials is the crystal engineering of novel materials based on inorganic molecules (Kayalvizhi et al. 2020). In general, inorganic NLO crystals possess high hyperpolarizability, optical transparency, thermal stability, resistance to optical damage, improved chemical stability, and good mechanical strength (Kayalvizhi et al. 2020; Kloda et al. 2019). Among the inorganic systems, borates are undoubtedly one of the most successful groups of NLO materials (Wang et al. 2004; Dhanuskodi et al. 2011). Boric acid is considered the preferred building block for the crystal engineering of organic and inorganic hybrid compounds (Malliga et al. 2020; Burgstaller et al. 2019). Also, nickel has been widely used for power control of electrical products, which is important for device miniaturisation and energy savings. Within a very diverse family of studied inorganic molecules, strong octahedral ligands of nickel (II) crystals have been reported (Reimann 1968). By employing this technique, it can be demonstrated that the crystal has the spherical shape, uniform size distribution, good crystallinity and high purity that are becoming more and more important for high-tech applications. (Wang et al. 2004). In this line of search, combination of nickel nitrate and boric acid can form new compounds with interesting NLO properties. A slow evaporation solution growth technique is used to prepare the title compound, nickel (II) nitrate hexahydrate boric acid (N2NHB). In this paper, we present the results of various analyses, including spectral, optical, SHG, SEM, EDAX, dielectric, photoconductivity and Z-scan studies, that have been performed on N2NHB to demonstrate that it is an excellent candidate for nonlinear optical applications in general.

2 Experimental section

2.1 Synthesis of N2NHB crystal

Nickel (II) nitrate hexahydrate and boric acid taken in a stoichiometric molar (1:1) ratio has been used to synthesise the nickel (II) nitrate hexahydrate boric acid. Figure 1 shows the chemical reaction that takes place. The calculated amount of reactants was thoroughly dissolved in aqueous solution, and there continuous stirring was done for 7 h to get a clear solution of the N2NHB precursor as homogeneous solution. The N2NHB solution was filtered off to remove insoluble impurities and transferred to a growing crystal chamber for slow evaporation at room temperature. The following is the synthesis scheme:

$$\left(\mathrm{Ni}\left(\mathrm{NO_3}\right)_2 \cdot 6\mathrm{H_2O}\right) + \left(\mathrm{H_3BO_3}\right) \rightarrow \left[\mathrm{Ni}\left(\mathrm{NO_3}\right)_2 \cdot 6\mathrm{H_2O} \cdot \mathrm{H_3BO_3}\right]$$

The grown crystal of N2NHB is depicted in Fig. 2. The photograph shows clear and transparent crystal with good dimensions that were grown within 4 weeks.

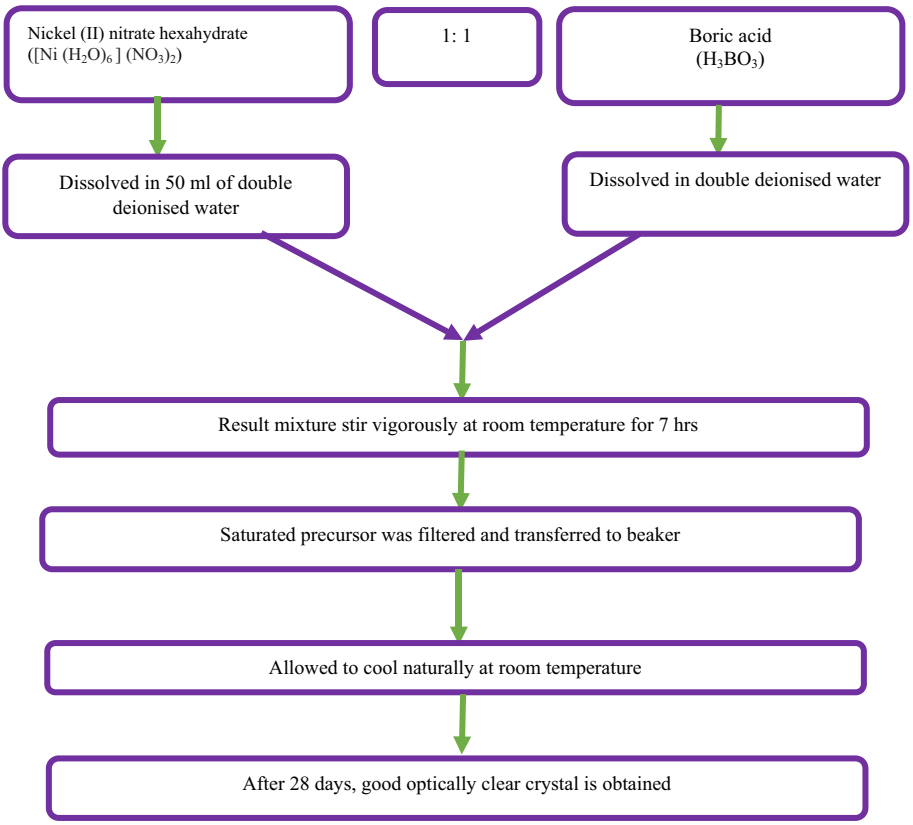

Fig. 1 The growing process of N2NHB single crystal

Fig. 2 As grown N2NHB crystal

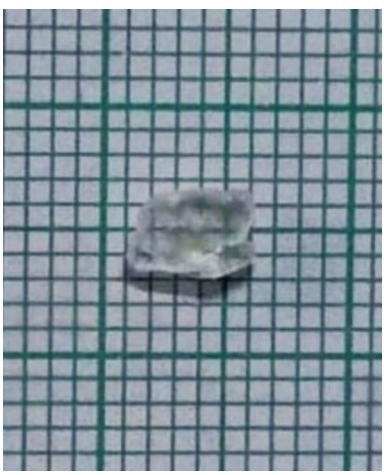

3 Results and discussion

3.1 Single crystal X-ray diffraction analysis

The crystals were subjected to crystal structure characterization using a Bruker Kappa ApexII CCD advance XRD instrument. The XRD peaks exposed that N2NHB crystallize in triclinic P crystal system, and the parameters of the lattices were obtained as a = 6.61 Å, b = 7.05 Å, c = 7.07 Å, α = 119.61°, β = 92.25°, γ = 101.11° and volume = 278 $Å^3$. The obtained cell parameter values differ from those of the pure boric acid cell parameter values (Lonappan 1955).

3.2 FTIR spectral analysis

A compound's structure can be better understood through vibrational interactions with the help of FTIR spectrum, which is a significant indicator of distinct functional groups. The different bands in a molecule stretch and bend in relation to one another when IR light is absorbed, respectively. The FTIR spectrum of N2NHB was recorded in the range 500–4000 cm^{-1} and is shown in Fig. 3. The peak at 3197 cm^{-1} indicates the presence of OH stretching vibrations (Kloda et al. 2019). The peak occurring at 2501 cm^{-1} have been assigned to N–H stretching vibrations (Kloda et al. 2019). The strong peak observed in the IR spectrum at 1405 cm^{-1} corresponds to B-O asymmetric stretching vibration (Joseph et al. 2003). The peak at 1189 cm^{-1} arises due to BO_3 stretching vibration (Shajan et al. 2016). BO_3 bending vibrations shows absorption bands at 880 cm^{-1} and 634 cm^{-1} (Kloda et al. 2019). The O–B–O and BOH bending vibrations were observed at 729 and 542 cm^{-1} respectively (Kloda et al. 2019; Shajan et al. 2016).

3.3 SEM and EDAX analysis

The surface of the grown sample crystal was investigated with a 'Quanta 200F' high-resolution scanning electron microscope' (SEM) with an accelerating voltage of 20 kV when the sample is in a vacuum state. Figure 4a–d shows the SEM pictographs in a highly effective and intuitive way and the size distribution and particle size of the synthesised N2NHB.

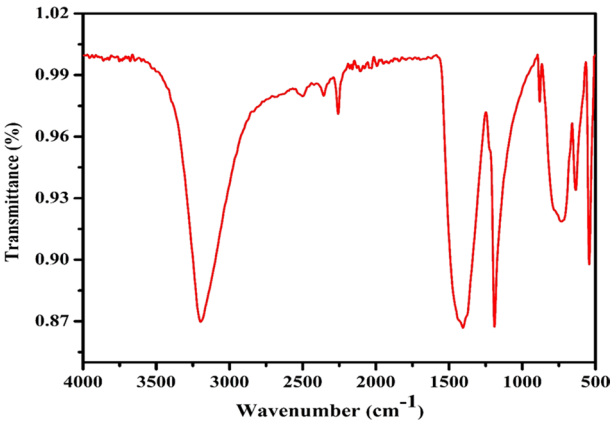

Fig. 3 FTIR spectrum of N2NHB crystal

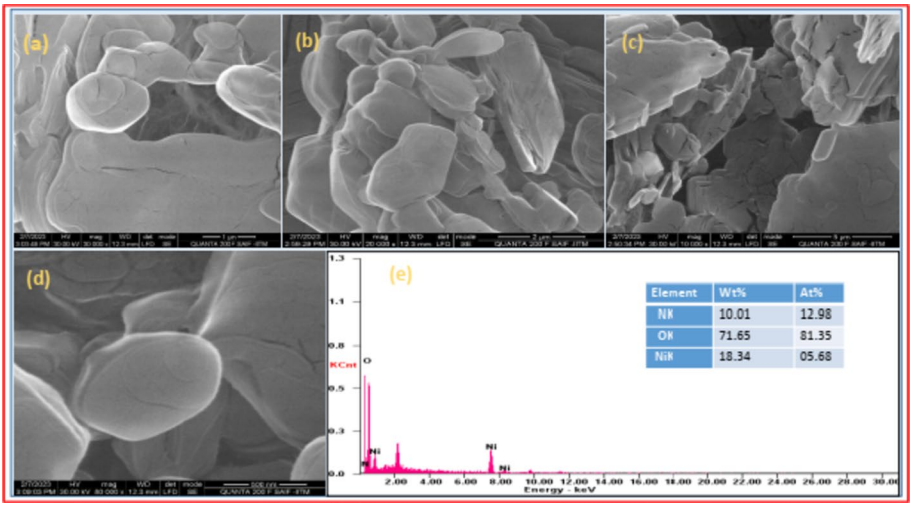

Fig. 4 **a–d** HR-SEM Micrographs of N2NHB crystal at different resolution **e** EDAX picture of grown N2NHB

According to the pictogram, the particles were nearly spherical in form. (Cao et al. 2020). From the SEM image, a little aggregation of particles can be seen. The EDAX graph (Fig. 5e) clearly confirms the presence of nickel in the grown crystal of N2NHB.

3.4 UV–visible studies

The absorption spectrum of the grown N2NHB sample was recorded from the range 200 to 800 nm using a UV–visible spectrometer. Due to the transfer of the electrons from the ground state to their excited energy states during the absorption of UV and visible light, the absorption spectrum provides crucial structural data (Shanthi et al. 2022). From the UV–visible spectrum of N2NHB (Fig. 5a), the absorption is very minimal in the visible region. The cut-off wavelength of N2NHB was identified at 314 nm, suggesting that the

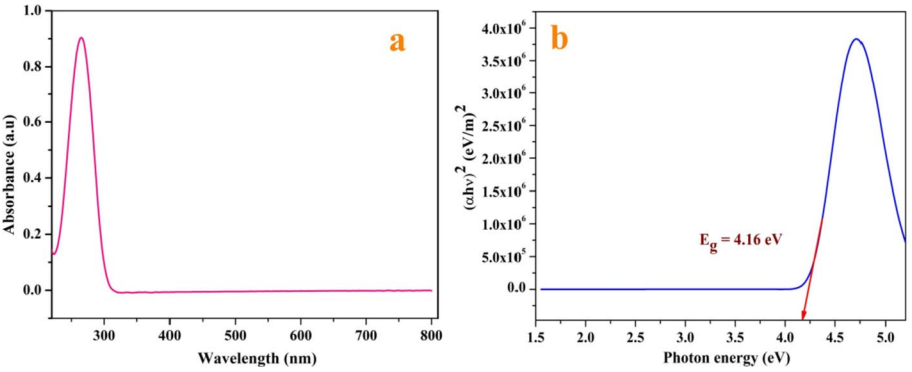

Fig. 5 **a** UV–visible spectrum and (**b**) Tacu's plot of N2NHB crystal

grown N2NHB is suitable for making optoelectronic devices to produce violet colour using a laser diode (Shenbagarajan et al. 2023).

The equation is used to calculate the optical absorption coefficient (α) and the energy band gap (Jayaprakash et al. 2017).

$$\alpha = \frac{2.303 \log\left(\frac{1}{T}\right)}{t} \tag{1}$$

where T is the fraction of transmitted light and t is the sample thickness. Direct band gap in transition materials,

$$h\nu\,\alpha = A(h\nu - Eg)^{1/2} \tag{2}$$

where 'h' refers to Planck's constant, 'ν' is the frequency of the incident photon, and A is the proportionality constant. Using the linear portion of the Tauc's plot (shown in Fig. 5b), the band gap of the N2NHB single crystal is calculated as 4.16 eV. The energy gap expands as the number of defects in a crystal is decreased (Shenbagarajan et al. 2023). The observed optical properties suggest that N2NHB single-crystal finds attractive use in NLO devices and UV-tunable lasers.

3.5 Photoluminescence (PL) study

The PL spectrum of N2NHB was analysed using a Perkin-Elmer LS 45 spectrofluorometer, and the excitation source used was a xenon arc lamp (450 W) (Shenbagarajan et al. 2023). PL can provide information about particular molecules present in grown crystals, including shallow and deep-level defects and gap-states (Jayaprakash et al. 2017). From this spectrum, the grown crystal N2NHB has one sharp, high-intensity peak at 533 nm is shown in Fig. 6. These obtained sharp emission peak, corresponds to green emission. The materials with a fluorescence peak of green emission have been found, and they will be more useful for LCD and OLED applications (Shenbagarajan et al. 2023).

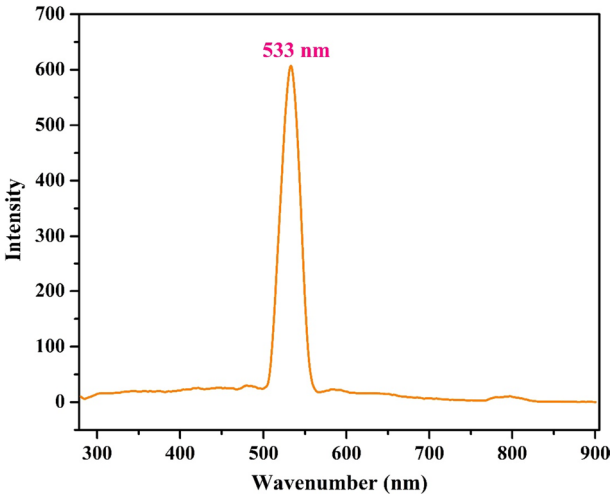

Fig. 6 Emission spectrum of grown N2NHB crystal

Further the observed green emission state avails pre-requisite for near-resonant state that leads to excited state absorption under green laser excitation.

3.6 Dielectric analysis

One of the most effective techniques to demonstrate the characterization of the electrical response of solids is through the use of dielectric measurements. Basically, polarisation mechanisms are available for the dielectric materials, divided into four types: electronic, ionic, orientation, and space charge polarization. To examine the sample lattice vibrations and carrier transport, dielectric investigations were conducted. The dielectric measurements of grown N2NHB crystals at various temperatures (313 K, 333 K, 353 K, and 373) were conducted using an HP multifrequency LCR metre in the frequency range of 50 Hz–5 MHz. The original part of the dielectric constant (ε′) and imaginary part of the dielectric constant (ε″) of the crystal have been evaluated by using these formula

$$\varepsilon' = \frac{Ct}{A\varepsilon_0} \tag{3}$$

$$\varepsilon'' = \varepsilon' \tan\delta \tag{4}$$

where C capacitance of the sample, D crystal thickness, ε_o permittivity in free space, A area of cross section of the grown sample, δ dielectric loss angle.

Figure 7a, b show the variation of the dielectric constant and the dielectric loss with frequency, respectively, for N2NHB-grown crystal at various temperatures. At very low applied frequencies, all types of polarisations will contribute to produce high dielectric constant. But the dielectric constant falls sharply at higher frequencies as electronic polarisation alone contributes to the dielectric constant at ultra-high frequencies, (Shenbagarajan et al. 2023). Other types of polarisation, such as space-charge and orientation polarisations, do not respond at high frequencies.

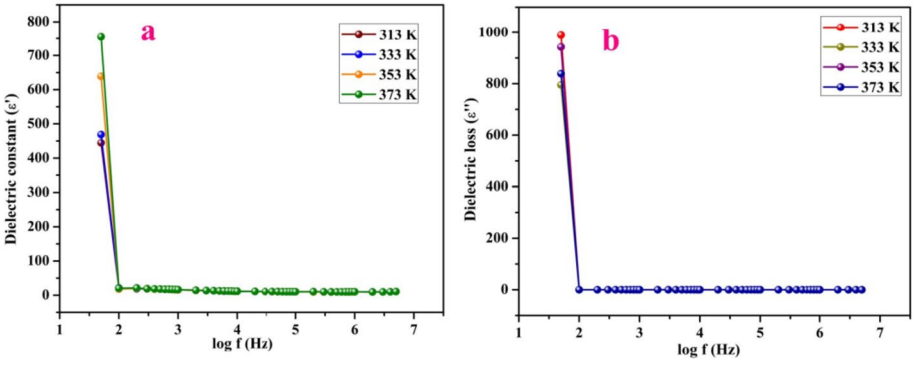

Fig. 7 **a** Variation of Dielectric constant at different Temperature. **b** Variation of Dielectric loss at different Temperature for N2NHB crystal

3.7 Photoconductivity studies

The photoconductivity studies of N2NHB grown crystal was made using Keithley 485 pm (Dhatchaiyini et al. 2019). The N2NHB sample was exposed to radioactive rays; the input voltage was a 100W halogen bulb, and the same object current was calculated. Figure 8 shows that the plotted curve between dark current and photo current increases with the applied field. These curves prove that dark current is less than photoelectric current. The positive photo conducting effect has wide application in mobile charge carriers because of the absorption of photons. The N2NHBgrown crystal have positive photoconductivity and are useful in optoelectronics and semiconductor laser applications.

3.8 Nonlinear optical (NLO) study

By using a Q-switched Nd: YAG laser with a fundamental beam of 1064 nm, it is possible to discover the second harmonic generation (SHG) property of the N2NHB crystal (Kayalvizhi et al. 2020). An airtight microcapillary tube with a consistent bore measuring approximately 1.5 mm in diameter was filled with the powder sample. The IR reflector was used to focus a laser beam that was then aimed at the microcrystalline powdered sample. The SHG radiation of 532 nm (green light) was collected by a photomultiplier tube (PMT, Hamamatsu model R 2059) and compared with potassium dihydrogen phosphate (KDP). From that, the SHG relative efficiency of nickel II nitrate hexahydrate boric acid crystal was 0.8 times that of KDP (Kloda et al. 2019).

3.9 Z-scan analysis

When analysing nonlinear optical phenomena like excited state absorption (ESA), two-photon absorption (2PA), and reverse saturable absorption (RSA), the Z-scan method is more accurate. (Natarajan et al. 2023). These tool measures the nonlinear absorption properties to identify the materials suitability for optical limiting applications that allows laser beam control to avoid laser induced damages (Jaikumar et al. 2020). Here Q-switched

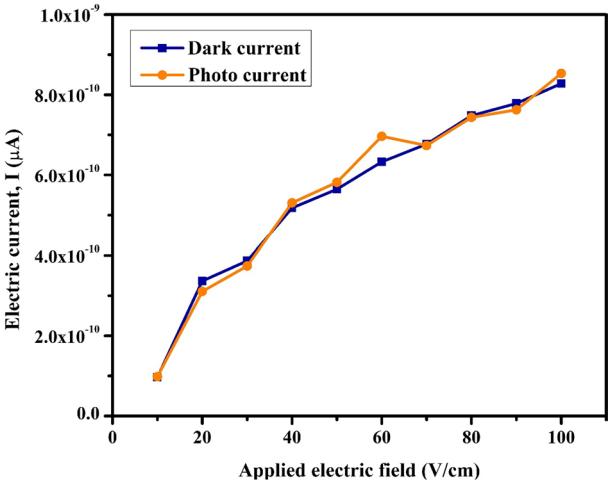

Fig. 8 Plot for photo current/dark current vs applied electric field for N2NHB

Nd:YAG laser with wavelength of 532 nm, pulse energy of 100 μJ and a pulse width of 9 ns was used as excitation source (Natarajan et al. 2023; Shalini et al. 2023). In this experiment, a focused Gaussian laser beam influence excitation of molecules. A quartz cuvette with a route length of 1 mm (the thickness of the sample) and a linear transmittance of 70% was used to sonicate the grown N2NHB crystal in ethanol (Shalini et al. 2023). The sample was moved along z-axis toward focal point (positive z-axis) and against (negative z-axis) and intensity of transmitted beam through moving the sample was measured as a function of position (Natarajan et al. 2023; Lima Rose et al. 2023). The Gaussian beam provide different level of laser intensity at different positions with the focus attaining highest levels. A graph was drawn between position (z) and normalized transmittance. Figure 9a shows the recorded open aperture Z-scan pattern of N2NHB (Jaikumar et al. 2020; Girisun and Dhanuskodi 2009). The presence of valley shaped curve symmetric about the focus point (z = 0) illustrates nonlinear reverse saturable absorption. Saturable absorption made a negligible contribution when the Z-scan data was fitted to several nonlinear transmission equations to determine the particular nonlinearity. In the curve fitting process, the effective nonlinear absorption coefficient is given by the relation

$$\alpha(I) = \left[\alpha_0/\left(1 + I/I_s\right) + \beta_{eff}I\right] \tag{5}$$

Here I_s stands for saturation intensity, α(I) for the intensity-dependent absorption coefficient, and α_0 for the linear absorption coefficient. The effective 2PA nonlinear coefficient was termed by the β_{eff}. The specific nonlinearities are here determined using two photon absorption (2PA), which provides a considerable contribution compared to the saturable absorption. The transmitted intensity, which is connected to an input intensity, is determined by the propagation equation:

$$dI/dz\prime = -\left[\alpha_0/\left(1 + I/I_s\right) + \beta I\right]I \tag{6}$$

We obtained the NLO coefficients from the graph by fitting Z-Scan data to a widely used NLO transmission equation. Based on the examination of the experimental data's best-fit curve, the nonlinear absorption coefficient and saturation intensity have been determined, and their respective values are 0.75×10^{-11} m/W and 50×10^{11} W/m^2, respectively. Optical tests revealed that the substance had a UV absorbance band (314 nm) and a green emission

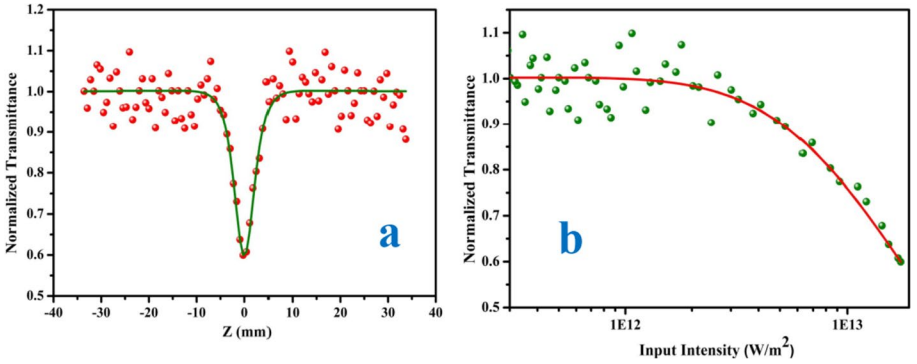

Fig. 9 **a** Z-scan curve for N2NHB. **b** Optical limiting curve for N2NHB

peak (533 nm). Under green laser excitation, these states act as 2PA state (314 nm) and near-resonant state (533 nm), resulting in excited state absorption. As a result, N2NHB displays sequential photon absorption. By absorbing the first photon, electrons are first propelled into the green emission state in this process. Then, by absorbing the second photon, they are propelled into the UV band. This typical behaviour of excited state absorption is attributed to sample-level optical limiting action (Habeebaa et al. 2021). The optical limiting graph drawn between transmittance and input fluence is shown in Fig. 9b. For a filtered Gaussian laser beam, the fluence (F (z)) at any point Z is expressed by an equation using the open aperture Z-scan data as

$$F(Z) = 4(\ln 2)^{1/2} E_{\text{in}} / \pi^{3/2} \left(z^2\right) \tag{7}$$

E_{in} stands for the input laser light's energy from the curve. The onset optical limiting threshold of N2NHB was measured to be 4.72×10^{12} W/m^2. Results show that N2NHB crystals have a low onset optical limiting threshold and a high two-photon absorption coefficient, making them an ideal material for laser safety devices. Table 1 represents the laser parameter of N2NHB single crystal.

4 Conclusion

Four weeks were taken to grow N2NHB crystals by the slow evaporation method from the homogeneous solution. The lattice parameters and volume of the orthorhombic crystal structure were found from the single-crystal X-ray diffraction study of the grown crystal. FT-IR analysis reveals the presence of various functional groups of the grown crystal. The SEM pictures were taken at different zooms (1 µm, 2 µm, 5 µm and 500 nm), and the EDAX graph shows the presence of nickel inside the grown crystal. The UV–visible spectra of the N2NHB crystal showed that it is highly transparent in the visible region, with a cut-off wavelength of 314 nm. Using Tauc's plot, the calculated optical band-gap value was found to be 4.16 eV. The fluorescence spectrum shows the emission peak at 533 nm, which corresponds to the green colour emission. The dielectric study reveals that the dielectric constant and dielectric loss decrease with increasing frequency at different temperatures. N2NHB second harmonic generation (SHG) performance is 0.8 times better than KDP. An investigation into photoconductivity revealed that the grown crystal has a photocurrent that is in the positive direction. The method of open-aperture Z-scanning was used in the

Table 1 Z-scan measurement for N2NHB single crystal

Laser parameters	Numerical values
Wavelength	532 nm
Frequency	10 Hz
Pulse width	9 ns
Beam waist	17 µm
Path length	1 mm
Rayleigh range	1.69 mm
Focal point	15 cm
Nonlinear absorption coefficient (β)	0.75×10^{-11} m/W
Intensity of saturation (I_s)	50×10^{11} W/m^2
Optical limiting threshold	4.72×10^{12} W/m^2

computation of the third-order nonlinear coefficient. According to the findings of the optical limiting investigation, N2NHB crystal are an excellent choice for usage in a variety of optical limiting applications.

Acknowledgements The authors would like to extend their heartfelt gratitude to SAIF IIT, Madras, for being helpful with the XRD experimentation. In addition, we would like to express our gratitude to the Department of Physics at BS Abdur Rahman University (BSAU), which is located in Chennai, for supplying the SHG analysis measurement equipment.

Author contributions V. Selvarani & P. Shenbagarajan: Conceptualization, Formal analysis, Writing -original draft, Data curation, Visualization. P. Jayaprakash: Formal analysis, Visualization, Investigation, Validation, Writing—review & editing. P. Ravichandran: Conceptualization, Methodology, Writing—review & editing, Validation, Investigation. T. C. Sabari Girisun & S. Selvaraj: Writing—review & editing, Resources, Methodology.

Funding The authors declare that no funds, grants, or other support were received during the preparation of this manuscript.

Data availability The authors declared that the data used in this paper is not used by any research work not shared to any instutition/agenecy**.**

Declarations

Conflict of interest The authors declare that this paper is not having any conflict of interest.

Ethical approval The authors declared that no compliance and ethical standard for this paper and work.

References

Burgstaller, M., Wurst, K., Huppertz, H.: Synthesis of the first nickel borate nitrate K7Ni[B18O24(OH)9](NO3)6· (H3BO3). Z. Naturforsch. **74**(10), 757–764 (2019)

Cao, L., Dai, P., Tang, J., Li, D., Chen, R., Liu, D., Gu, X., Li, L., Bando, Y., Ok, Y.S., Zhao, X., Yamauchi, Y.: Spherical superstructure of boron nitride nanosheets derived from boron-containing metal-organic frameworks. J. Am. Chem. Soc. **142**(19), 8755–8762 (2020). https://doi.org/10.1021/jacs.0c01023

Dhanuskodi, S., Sabari Girisun, T.C., Bhagavannarayana, G., Uma, S., Phillip, J.: Mechanical, thermal and laser damage threshold analyses of II group metal complexes of thiourea. Mater. Chem. Phys. **126**(3), 463–469 (2011). https://doi.org/10.1016/j.matchemphys.2011.01.024

Dhatchaiyini, M.K., Rajasekar, G., Bhaskaran, A.: Synthesis, growth, optical, photoconductivity and specific heat properties of potassium borodicitrate (KBDC) single crystal. J. Mater. Sci. **54**, 9362–9371 (2019). https://doi.org/10.1007/s10853-019-03542-4

Girisun, T.C.S., Dhanuskodi, S.: Linear and nonlinear optical properties of tris-thiourea zinc sulphate single crystals. Cryst. Res. Technol. **12**, 1297–1302 (2009). https://doi.org/10.1002/crat.200900351

Habeebaa, A.A.U., Saravanan, M., Girisunb, T.C.S., Anandana, S.: Nonlinear optical studies of conjugated organic dyes for optical limiting applications. J. Mol. Struct. **1240**, 130559 (2021). https://doi.org/10.1016/j.molstruc.2021.130559

Jaikumar, P., Balakrishnan, T., Indumathi, C., Girisun, T.C.S., Ramamurthi, K.: Nonlinear optical behaviour of bis (cytosinium) tartarate monohydrate single crystal. Chem. Phys. Impact **5**, 100114 (2020). https://doi.org/10.1016/j.chphi

Jayaprakash, P., Sangeetha, P., Kumari, C.R.T., Caroline, M.L.: Investigation on the growth, spectral, lifetime, mechanical analysis and third-order nonlinear optical studies of L-methionine admixtured D-mandelic acid single crystal: a promising material for nonlinear optical applications. Phys. B Condens. Matter **518**, 1–12 (2017). https://doi.org/10.1016/j.physb.2017.05.017

Joseph, V., Gunasekaran, S., Santhanam, V.: Photoconductivity and dielectric studies of potassium pentaborate crystal (KB5). Bull. Mater. Sci. **26**, 383–386 (2003). https://doi.org/10.1007/BF02711180

Kayalvizhi, C., Anand, S., Durga, R., Ebinezer, B.S., Sundararajan, R.S.: Structural, vibrational and optical studies on semi organic crystals of boric acid potassium acetate. Heliyon **6**, e03133 (2020). https://doi.org/10.1016/j.heliyon.2019.e03133. (**PMID: 32042942; PMCID: PMC7002783**)

Kloda, M., Matulkova, I., Clsarova, I., Becker, P., Bohaty, L., Nemec, P., Gyepes, R., Nemec, I.: Cocrystals of 2-aminopyrimidine with boric acid—crystal engineering of a novel nonlinear optically (NLO) active crystal. Crystals **9**(8), 403 (2019). https://doi.org/10.3390/cryst9080403

Lima Rose, M.L., Suthan, T., Gnanasambandam, C., et al.: Growth and characterization of organic 2,3,4-trihydroxybenzophenone single crystals for nonlinear optical applications. J. Mater. Sci. Mater. Electron. **34**, 884 (2023). https://doi.org/10.1007/s10854-023-10224-0

Lonappan, M.A.: Thermal expansion of boric acid. Proc. Indian Acad. Sci. **42**, 10–21 (1955). https://doi.org/10.1007/BF03053556

Malliga, P., Dharshan, V., Deepika, V.: Synthesis, growth and optical characterisation of nickel added Boro Formate single crystal for optical applications. J. Phys. (2020). https://doi.org/10.1088/1742-6596/1706/1/012001

Natarajan, R., Ebinezer, B.S., Sundararajan, R.S., et al.: Synthesis and characterization of L-asparagine monohydrate potassium dichromate (LAMPDC): novel material for optical limiting applications. J. Mater. Sci. Mater. Electron. **34**, 970 (2023). https://doi.org/10.1007/s10854-023-10408-8

Reimann, C.W.: The single crystal spectrum of hexakis(imidazole)nickel(II)Nitrate. J. Res. Natl. Bur. Stand. A Phys. Chem. **72A**(6), 765–768 (1968). https://doi.org/10.6028/jres.072a.050. (**PMID: 31824120; PMCID: PMC6696561**)

Shajan, D., Murugasen, P., Sagadevan, S.: Analysis on the structural, spectroscopic, and dielectric properties of borate glass. Dig. J. Nanomater. Biostruct. **11**, 177–183 (2016)

Shalini, M., Sundararajan, R.S., Manikandan, E., Meena, M., Ebinezer, B.S., Girisun, T.C.S., Natarajan, R.: Growth and characterization of L-Methionine Barium Bromide (LMBB)semi-organic crystal for optical limiting applications. Optik **278**, 17075 (2023). https://doi.org/10.1016/j.ijleo.2023.170705

Shanthi, C., Jayaprakash, P., Sagayaraj, P., Kubendiren, T., Ravisankar, R.: Crystal growth and physicochemical characterizationof a semi-organic L-glutamic acid manganese chloride single crystal for nonlinear optical applications. J. Mater. Sci. Mater. Electron. **33**, 18124–18133 (2022). https://doi.org/10.1007/s10854-022-08670-3

Shenbagarajan, P., Jayaprakash, P., Krishnan, S., Selvaraj, S., Sabari Girisun, T.C.: An extensive investigation of the structural, spectral, optical, electrical, and nonlinear optical properties of a single crystal of Di-aqua nitrato bis L-valine Lead (II) Nitrate. Opt. Mater. **144**, 114337 (2023). https://doi.org/10.1016/j.optmat.2023.114337

Wang, W.N., Itoh, Y., Lenggoro, I.W., Okuyama, K.: Nickel and nickel oxide nanoparticles prepared from nickel nitrate hexahydrate by a low pressure spray pyrolysis. Mater. Sci. Eng. **111**(1), 69–76 (2004). https://doi.org/10.1016/j.mseb.2004.03.024